Tetrahedron 65 (2009) 7491–7497

Contents lists available at ScienceDirect

Tetrahedron

journal homepage: www.elsevier.com/locate/tet

Mechanism of the α,α-diarylprolinol trimethylsilyl ether-catalyzed enantioselective C–C, C–N, C–F, C–S, and C–Br bond forming reactions

Chiong Teck Wong

*Institute of High Performance Computing (IHPC), Agency for Science, Technology and Research (A*STAR) 1 Fusionopolis Way, #16-16 Connexis, Singapore 138632, Singapore*

ARTICLE INFO

Article history:
Received 1 March 2009
Received in revised form 24 June 2009
Accepted 2 July 2009
Available online 8 July 2009

ABSTRACT

Theoretical calculations were employed to investigate the enantioselectivity of the α,α-diarylprolinol trimethylsilyl ether-catalyzed α-functionalization of aldehydes with various different electrophiles, via an enol intermediate. The reactions investigated were (i) Michael–aldol condensation, (ii) Michael addition, (iii) Mannich reaction, (iv) α-amination of an aldehyde, (v) α-fluorination of an aldehyde, (vi) α-sulfenylation of an aldehyde, and (vii) α-bromination of an aldehyde. In all seven cases, our proposed enol mechanism is able to account for the experimentally observed enantioselectivity of the products. Our calculations strongly suggest that these catalyzed reactions proceed via an enol intermediate and not via an enamine intermediate.

1. Introduction

The α,α-diarylprolinol trimethylsilyl ether ((*S*)-**Cat**) molecule (Fig. 1) is a versatile organocatalyst, which is employed in enantioselective C–C, C–N, C–F, C–S, and C–Br bond formations.[1–4] These (*S*)-**Cat**-catalyzed reactions are commonly assumed to proceed via an enamine intermediate.[1b,c,3] Theoretical studies on the stereoselectivity of the (*S*)-**Cat**-catalyzed reactions also make such an assumption.[5] The enamine mechanism is extended from the case of the proline-catalyzed aldol reaction.[6] Although enamine intermediates have never been detected experimentally in the proline-catalyzed aldol reactions, experimental[7] and theoretical[8] studies seem to support indirectly the enamine pathway. We note here that in List et al.,[7a] NMR spectroscopic studies of the reaction between acetone and proline, report the formation of oxazolidinone instead of enamine. Recently, Yalalov et al.[9] presented experimental evidence for an enol mechanism in a primary amine–thiourea (organocatalyst) catalyzed Mannich-type reaction.

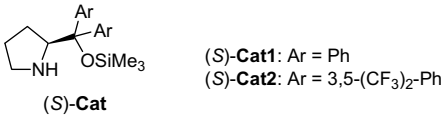

Figure 1. The α,α-diarylprolinol trimethylsilyl ether ((*S*)-**Cat**) catalyst.

In the enamine mechanism, the first step of enamine formation between an amine and an aldehyde involves C–N bond formation between the carbonyl carbon of the aldehyde and the nitrogen of the amine-catalyst. Organocatalysts that contain acidic hydrogens will facilitate the C–N bond formation step, as in the case of the proline-catalyzed aldol reaction.[8d] Organocatalysts that do not contain acidic hydrogens usually employ additives[1a,4] (e.g., carboxylic acids) in the reaction, probably to promote enamine formation.

Interestingly, despite the absence of acidic hydrogens in (*S*)-**Cat**, it is able to catalyze C–C, C–N, C–F, C–S, and C–Br bond formation without the need for additives.[1] We suspect that these (*S*)-**Cat**-catalyzed reactions may not proceed via an enamine intermediate and this has led us to investigate the (*S*)-**Cat1**-catalyzed oxyamination reaction.[10] In that study, we considered four plausible initial reactions between (*S*)-**Cat1** and butanal (Scheme 1). Our theoretical calculations revealed that the reaction leading to enol formation (via **TSd**) is energetically favored, which strongly suggests that the (*S*)-**Cat1**-catalyzed oxyamination reaction proceeds via an enol intermediate and not via an enamine intermediate. We have proposed the following enol mechanism[10] for (*S*)-**Cat**-catalyzed reactions (Scheme 2): (i) (*S*)-**Cat** reacts with an aldehyde to generate a *trans* enol tautomer, and forms a *trans* enol-catalyst hydrogen bonded complex. (ii) A reactant molecule subsequently reacts with the *trans* enol–catalyst complex (Fig. 2) to afford an enantioselective product.

To further validate our proposed enol mechanism (Scheme 2) for this class of organocatalyst, we report here our investigations on the enantioselectivity of (*S*)-**Cat**-catalyzed C–C, C–N, C–F, C–S, and C–Br bond forming reactions (Scheme 3).

E-mail address: wongct@ihpc.a-star.edu.sg

0040-4020/$ – see front matter © 2009 Elsevier Ltd. All rights reserved.
doi:10.1016/j.tet.2009.07.008

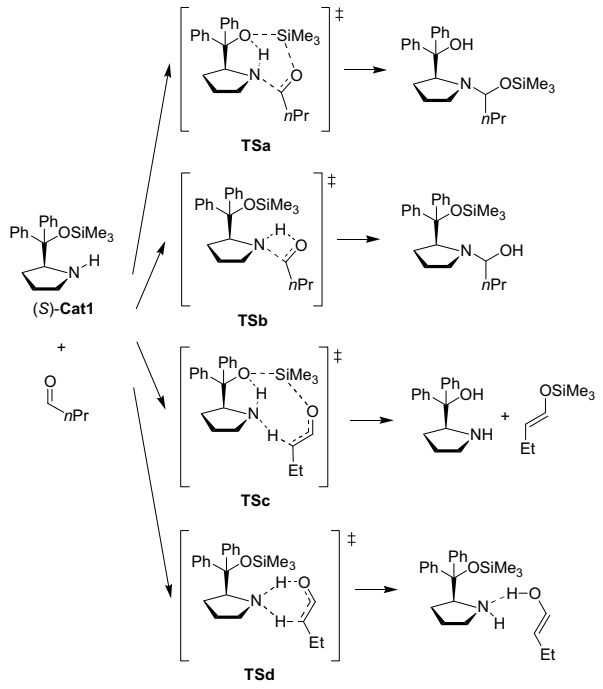

Scheme 1. Plausible initial reactions between (*S*)-**Cat1** and butanal.[10]

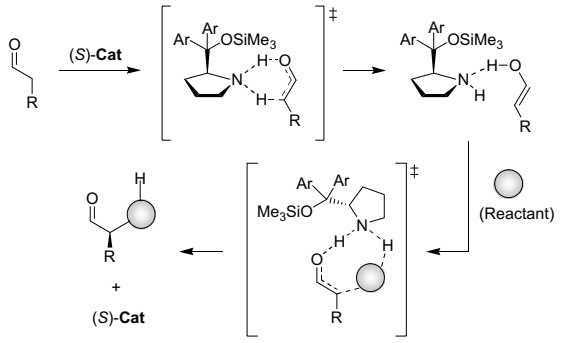

Scheme 2. Proposed mechanism for enantioselective (*S*)-**Cat**-catalyzed reactions.[10]

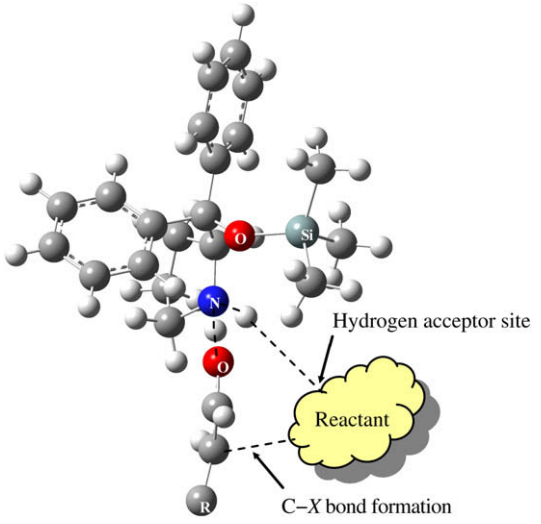

Figure 2. Transition state depicting the reaction between the *trans* enol–catalyst complex and a reactant molecule, to afford an enantioselective product.

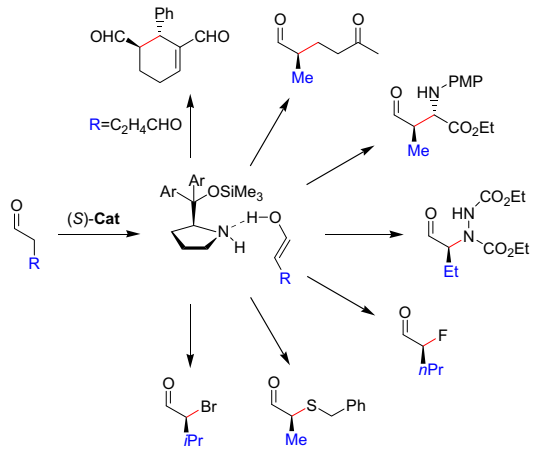

Scheme 3. (*S*)-**Cat**-catalyzed C–C, C–N, C–F, C–S, and C–Br bond forming reactions[1a,c] investigated in this study.

2. Computational methods

Geometry optimizations were performed using the B3LYP[11] hybrid density functional theory method with the 6-31G* basis set for all molecular structures. All optimized geometries were verified to be equilibrium structures or transition states via frequency calculations. An equilibrium structure will have all real frequencies while a transition state will have one and only one imaginary frequency. The effect of solvent was studied using the polarization continuum model (PCM).[12] The solvation sphere size (ALPHA value) was set to 1.50 as this value is required to achieve optimization convergence for some transition states. The calculated energies were improved through MP2/6-311G** single-point energy solvation (PCM) calculations. Unless otherwise noted, all energies (ΔE and $\Delta E^{\ddagger}$) reported are in kJ mol^{-1} and correspond to MP2/6-311G**(PCM)//B3LYP/6-31G*(PCM), including B3LYP/6-31G*(PCM) zero-point energy (scaled). A scaling factor of 0.9804[13] was used to correct for the directly computed B3LYP/6-31G*(PCM) zero-point energies. All calculated enthalpy energies (ΔH and $\Delta H^{\ddagger}$) reported are in kJ mol^{-1} and correspond to B3LYP/6-31G*(PCM) at the respective reaction temperature. All calculated Gibbs free energies (ΔG and $\Delta G^{\ddagger}$) reported are in kJ mol^{-1} and correspond to B3LYP/6-31G*(PCM) at the respective reaction temperature. All calculations were performed using Gaussian03.[14]

3. Results and discussions

3.1. Michael–aldol condensation (C–C bond formation)

The enantioselective domino Michael–aldol reaction between 5-oxoalkanal and α,β-unsaturated aldehydes, catalyzed by (*S*)-**Cat1**, has been reported by Hong et al.[1a] (Scheme 4). This reaction involves two C–C bond formation steps and affords cyclohexene product diastereomers containing two chiral centers, with high enantioselectivity of the *anti*-product.

For the reaction shown in Scheme 4, following our proposed enol mechanism (Scheme 5), pentane-1,5-dial (**R1a**) reacts with

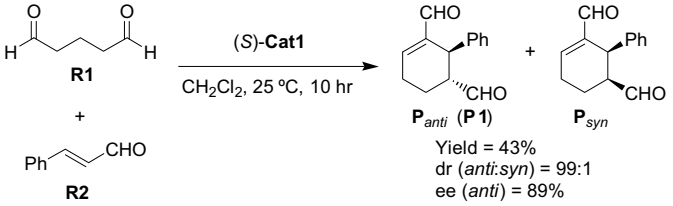

Scheme 4. Enantioselective domino Michael–aldol reaction catalyzed by (*S*)-**Cat1**.[1a]

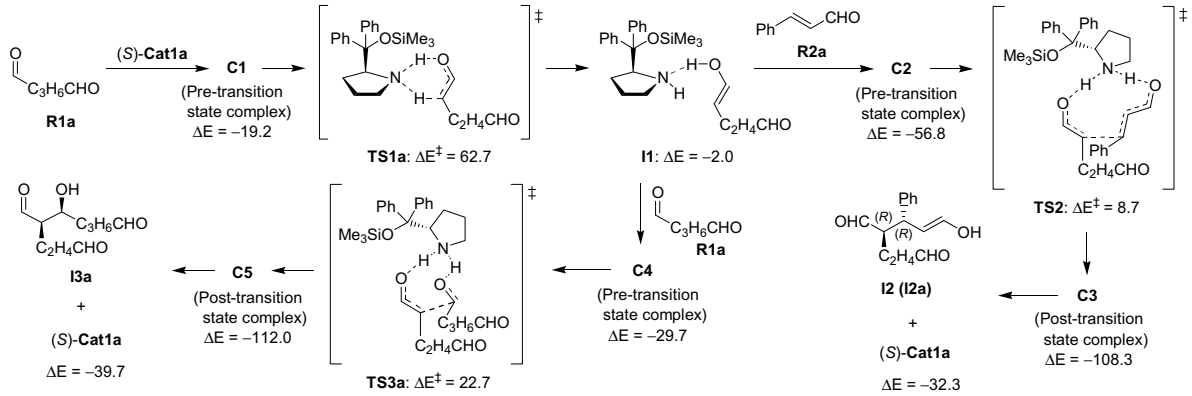

Scheme 5. Proposed reaction mechanism for the (*S*)-**Cat1**-catalyzed Michael reaction, via an enol intermediate. Calculated energy barriers ($\Delta E^{\ddagger}$) and reaction enthalpies (ΔE) correspond to the relative energy with respect to **R1a** (i.e., the free reactants), in kJ mol^{-1}.

(*S*)-**Cat1a** (via **TS1a**) to form a *trans* enol–catalyst hydrogen bonded complex (**I1**). Formation of the *cis* enol–catalyst hydrogen bonded complex (via **TS1b**) is calculated to be 3.4 kJ mol^{-1} (MP2 value) higher in energy than **TS1a**.

The *Re* face of 3-phenylpropenal (**R2a**) subsequently reacts with **I1** (from the *Re* face of the *trans* enol moiety of **I1**) via **TS2** to form **I2a** (Fig. S1 in Supplementary data). Transition state **TS2** consists of simultaneous (i) C–C bond formation between enol and **R2a**, (ii) a H-shift from the O of enol to the N of (*S*)-**Cat1a**, and (iii) a H-shift from the N of (*S*)-**Cat1a** to the O of **R2a**. The reaction involving the *Si* face of the most stable conformer of 3-phenylpropenal (**R2a**) with **I1**, via a transition state that is analogous to **TS2**, is geometrically challenging.

Pentane-1,5-dial could also react with **I1** (via **TS3a**) to form a homo-aldol product **I3a**. The calculated MP2 energy barrier corresponding to **TS3a** is 22.7 kJ mol^{-1}, which is 14.0 kJ mol^{-1} higher in energy than the activation barrier corresponding to **TS2**.

Conformer **I2a** will undergo rotation(s) to conformer **I2b** where an intramolecular aldol reaction takes place between the enol and aldehyde functional groups (via **TS4a**) to afford intermediate **I4a** (Scheme 6). The transition state structure of **TS4a** adopts a cyclohexane chair conformation with the peripheral CHO and Ph groups situated at the equatorial positions to avoid steric effects at the axial positions. Transition state **TS4a** consists of simultaneous (i) C–C bond formation between the enol and aldehyde functional groups, and (ii) a H-shift from the O of enol to the O of aldehyde. The C–C bond formation and H-shift proceed via a six-membered cyclic structure, similar to that observed in the uncatalyzed aldol[10] and uncatalyzed Mukaiyama aldol reaction.[15]

Two transition states (**TS4b** and **TS4c**) analogous to **TS4a**, which afford the corresponding diastereomers of **I4a** were also located (Scheme 6). Their calculated energy barriers are at least 5.1 kJ mol^{-1} higher in energy than **TS4a**. The preference for the formation of **I4a** is attributed to the orientation of the 'larger' groups (i.e., the O of the aldehyde and the CHOH fragment of the enol moiety) in **TS4a**. These larger groups tend to adopt the equatorial positions of the forming cyclohexane ring in order to avoid 1,3-diaxial interactions, thus leading to a lower energy for transition state **TS4a**. The MP2 energy profile for the formation of **I3a**, **I4a**, **I4b**, and **I4d** is shown in Figure 3.

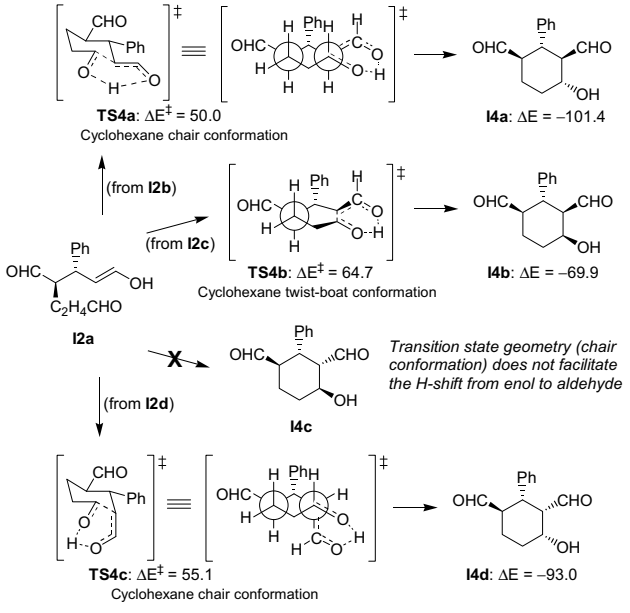

Scheme 6. Conformational analysis for the C–C bond formation in the aldol reaction. Calculated energy barriers ($\Delta E^{\ddagger}$) and reaction enthalpies (ΔE) correspond to the relative energy with respect to **I2a**, in kJ mol^{-1}. Compounds **I2a**, **I2b**, **I2c**, and **I2d** are conformational isomers.

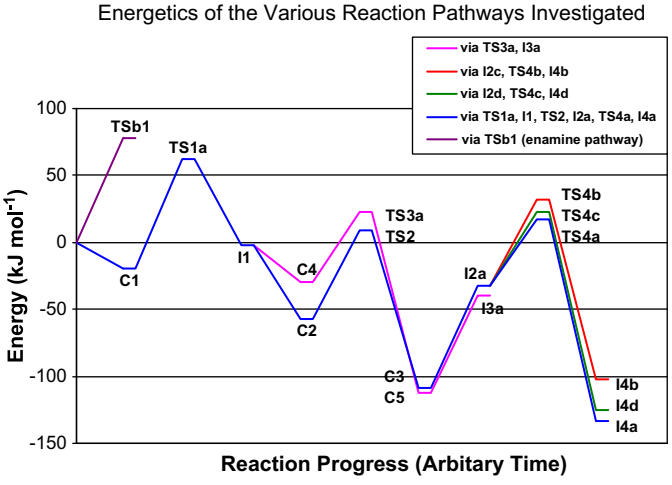

Figure 3. Calculated energy (MP2) profile for the formation of **I3a**, **I4a**, **I4b**, and **I4d**.

The dehydration of **I4a** can yield two possible products, **P1** and **P2** (Scheme 7). In the absence of an acid catalyst, a concerted elimination of a H_2O molecule (via **TS5**) to form **P2** is calculated to be 315.6 kJ mol^{-1}. The elimination of H_2O to obtain **P1** is found to proceed via a stepwise pathway involving intermediate **I5**, via **TS6** and **TS7**. The pathway leading to the formation of **P1** is calculated to be 101.2 kJ mol^{-1} lower in energy than the concerted pathway via **TS5**. This is in agreement with the experimental observation for the

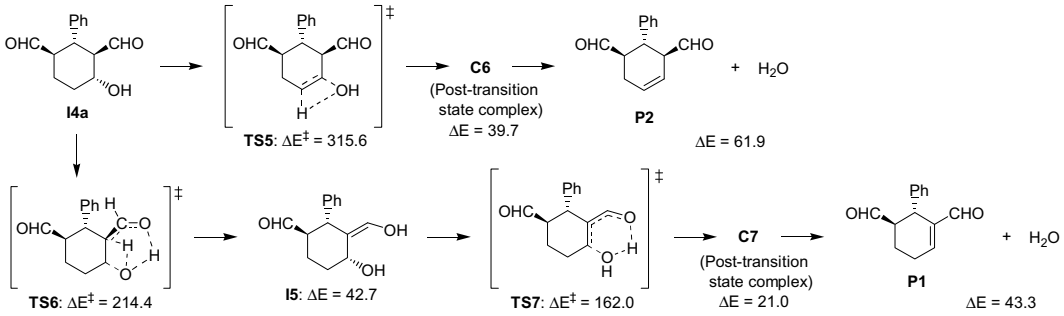

Scheme 7. Dehydration of **I4a**. Calculated energy barriers ($\Delta E^{\ddagger}$) and reaction enthalpies (ΔE) correspond to the relative energy with respect to **I4a**, in kJ mol^{-1}.

formation of **P1**. The proposed enol mechanism can fully account for the experimentally observed product diastereoselectivity and enantioselectivity.

3.2. Michael addition (C–C bond formation)

The (*S*)-**Cat2**-catalyzed Michael addition reaction between propanal and methylvinyl ketone (**R4**) has been reported by Franzén et al.[1c] (Scheme 8). Following our proposed enol mechanism (Scheme 9), the *trans* enol–catalyst complex (**I6**) reacts with **R4a** via **TS9** to afford intermediate **I7**. Transition state **TS9** consists of simultaneous (i) C–C bond formation between the enol and **R4a**, (ii) a H-shift from the O of the enol to the N of (*S*)-**Cat2a**, and (iii) a H-shift from the N of (*S*)-**Cat2a** to the O of **R4a**.

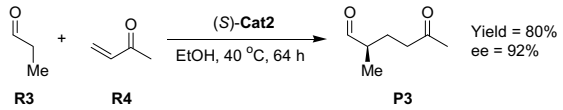

Scheme 8. (*S*)-**Cat2**-catalyzed Michael addition.[1c]

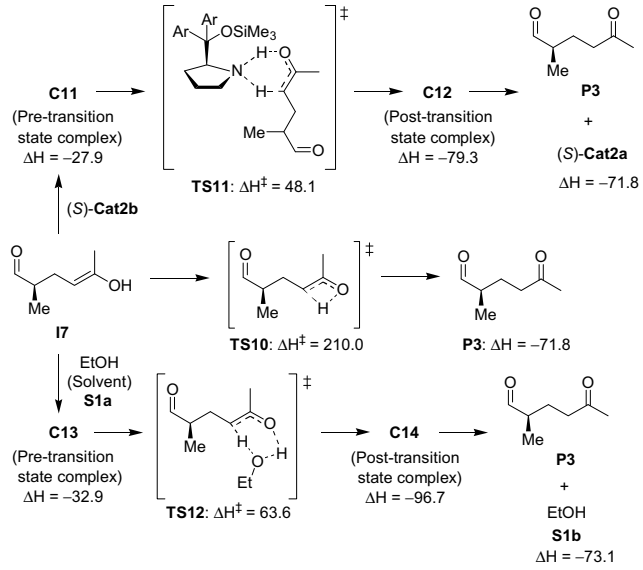

Scheme 10. Formation of **P3** from **I7**. Calculated enthalpy energies ($\Delta H^{\ddagger}$ and ΔH) correspond to the relative energy with respect to **I7**, in kJ mol^{-1}.

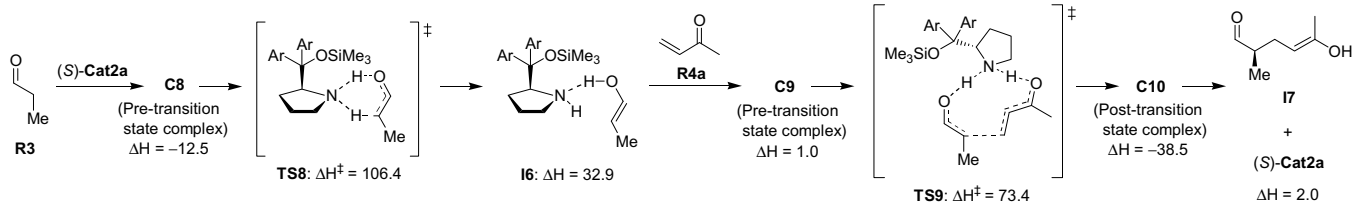

Scheme 9. Proposed reaction mechanism for the (*S*)-**Cat2a**-catalyzed Michael addition reaction, via an enol intermediate. Calculated enthalpy energies ($\Delta H^{\ddagger}$ and ΔH) correspond to the relative energy with respect to **R3** (i.e., the free reactants), in kJ mol^{-1}.

Compound **I7** subsequently reacts with (*S*)-**Cat2b** via **TS11** or alternatively may react with an ethanol solvent molecule (via **TS12**) to afford the experimentally observed Michael addition product **P3** (Scheme 10). The uncatalyzed isomerization reaction from **I7** to **P3**, via **TS10**, is calculated to be significantly higher in energy. The calculated reaction enthalpy profile is shown in Figure S4 (in Supplementary data).

3.3. Mannich reaction (C–C bond formation)

The (*S*)-**Cat2**-catalyzed Mannich reaction between propanal and **R6** is shown in Scheme 11. Following our proposed enol mechanism (Scheme 12), the *trans* enol–catalyst complex (**I8**) reacts with **R6** via **TS14a** to afford the experimentally observed product diastereomer **P4a**. Transition state **TS14a** consists of simultaneous (i) C–C bond formation between the enol and **R6**, (ii) a H-shift from the O of the enol to the N of (*S*)-**Cat2c**, and (iii) a H-shift from the N of (*S*)-**Cat2c** to the N

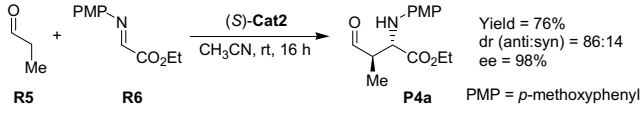

Scheme 11. (*S*)-**Cat2**-catalyzed Mannich reaction.[1c]

of **R6**. The formation of diastereomer **P4b**, via **TS14b**, is calculated to be 1.7 kJ mol^{-1} higher in energy than **TS14a**. We predict that the *syn* diastereomer product will primarily be that of **P4b**. The calculated reaction enthalpy profile is shown in Figure S5 (in Supplementary data).

3.4. α-Amination of an aldehyde (C–N bond formation)

The (*S*)-**Cat2**-catalyzed α-amination of butanal with **R8** affords **P6** after $NaBH_4$ reduction (Scheme 13). The first-formed product (prior to $NaBH_4$ reduction) is expected to be **P5**.

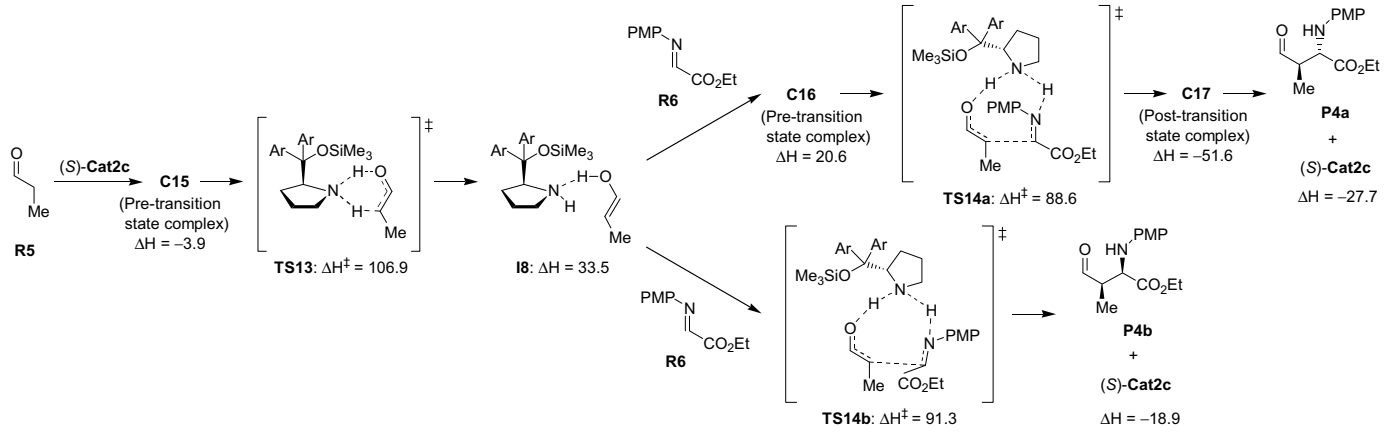

Scheme 12. Proposed reaction mechanism for the (*S*)-**Cat2c**-catalyzed Mannich reaction, via an enol intermediate. Calculated enthalpy energies ($\Delta H^{\ddagger}$ and ΔH) correspond to the relative energy with respect to **R5** (i.e., the free reactants), in kJ mol^{-1}.

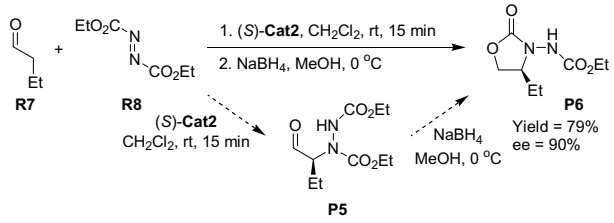

Scheme 13. (*S*)-**Cat2**-catalyzed α-amination of butanal.[1c]

Interestingly, our investigations revealed that the *trans* enol–catalyst complex (**I9**) reacts with **R8** via a stepwise pathway to afford the first-formed product **P5** (Scheme 14). Compound **I9** first reacts with **R8** via a H-shift from the O of the enol to the N of (*S*)-**Cat2d** (via **TS16**), to form a zwitterionic intermediate **I10**. Next, a C–N bond forming reaction occurs (via **TS17**) to yield another zwitterionic intermediate **I11**. The stability of the zwitterionic intermediates **I10** and **I11** may be attributed to resonance. Compound **I11** then undergoes a H-shift from the N of (*S*)-**Cat2d** to the O of **R8** (via **TS18**) to afford intermediate **I12**. An intramolecular H-shift subsequently occurs in **I12** via **TS19** to afford **P5** (Scheme 15), which will yield the experimentally observed product **P6** upon reduction with $NaBH_4$. The calculated reaction enthalpy profile is shown in Figure S6 (in Supplementary data).

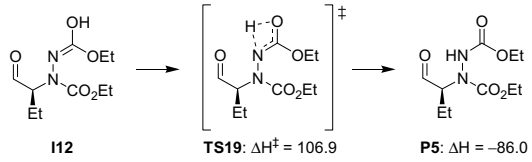

Scheme 15. Isomerization of **I12** to **P5**. Calculated enthalpy energies ($\Delta H^{\ddagger}$ and ΔH) correspond to the relative energy with respect to **I12**, in kJ mol^{-1}.

3.5. α-Fluorination of an aldehyde (C–F bond formation)

The (*S*)-**Cat2**-catalyzed α-fluorination of pentanal with **R10** affords **P8** after $NaBH_4$ reduction (Scheme 16). The first-formed product (prior to $NaBH_4$ reduction) is expected to be **P7**. Following our proposed enol mechanism (Scheme 17), the *trans* enol–catalyst complex (**I13**) reacts with **R10** via **TS21** to afford **P7** and **I14**. Transition state **TS21** consists of simultaneous (i) C–F bond formation

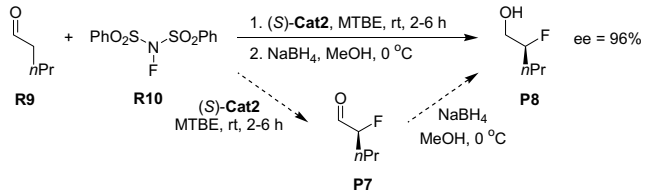

Scheme 16. (*S*)-**Cat2**-catalyzed α-fluorination of pentanal.[1c]

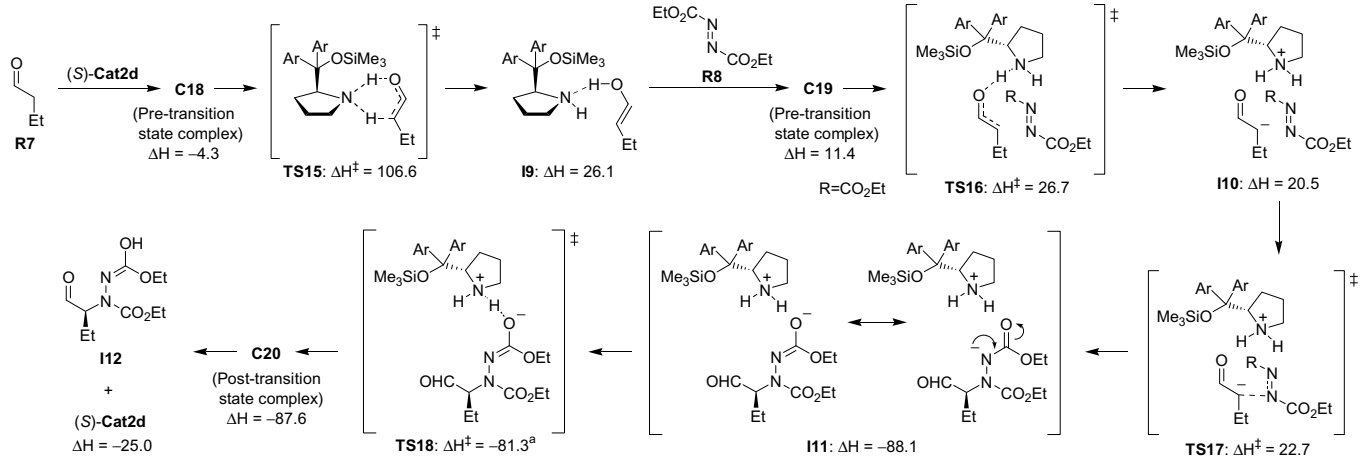

Scheme 14. Proposed reaction mechanism for the (*S*)-**Cat2d**-catalyzed α-amination of butanal, via an enol intermediate. Calculated enthalpy energies ($\Delta H^{\ddagger}$ and ΔH) correspond to the relative energy with respect to **R7** (i.e., the free reactants), in kJ mol^{-1}. [a]Estimated $\Delta H^{\ddagger}$ value from the difference between the calculated electronic energy of **TS18** and **I11**.

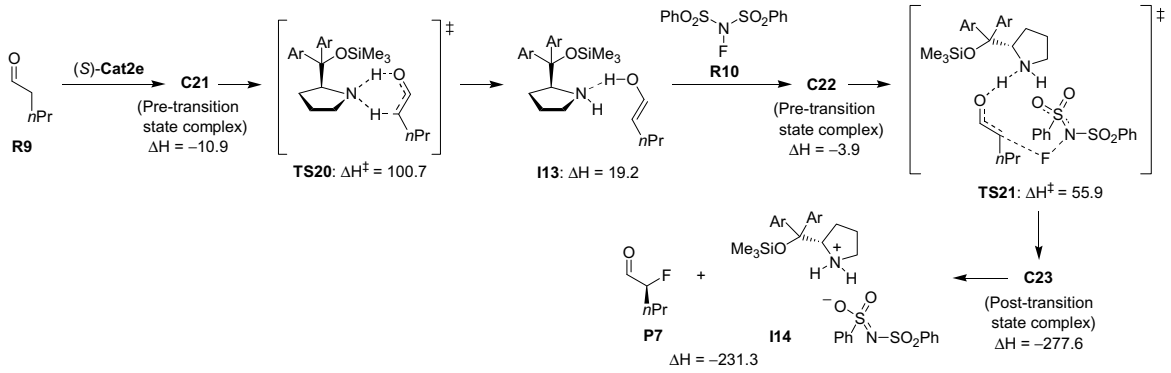

Scheme 17. Proposed reaction mechanism for the (*S*)-**Cat2e**-catalyzed α-fluorination of pentanal, via an enol intermediate. Calculated enthalpy energies ($\Delta H^{\ddagger}$ and ΔH) correspond to the relative energy with respect to **R9** (i.e., the free reactants), in kJ mol^{-1}.

between the enol and **R10** via a F-shift, and (ii) a H-shift from the O of the enol to the N of (*S*)-**Cat2e**. Subsequent reduction of **P7** with $NaBH_4$ will yield the experimentally observed product **P8**. Although **R10** is commonly viewed as a F^+ reagent,[16] the reaction between **I13** and F^+ was not considered as the heterolytic N–F bond dissociation in **R10** is highly unfavorable (Scheme 18). The calculated reaction enthalpy profile is shown in Figure S7 (in Supplementary data).

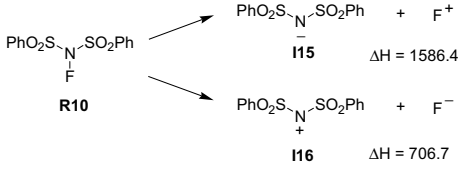

Scheme 18. Heterolytic N–F bond dissociation in **R10**. Calculated enthalpy energies (Δ*H*) correspond to the relative energy with respect to **R10**, in kJ mol^{-1}.

3.6. α-Sulfenylation of an aldehyde (C–S bond formation)

The (*S*)-**Cat2**-catalyzed α-sulfenylation of propanal with **R12** affords **P10** after $NaBH_4$ reduction (Scheme 19). The first-formed product (prior to $NaBH_4$ reduction) is expected to be **P9**. Following our proposed enol mechanism (Scheme 20), the *trans* enol–catalyst complex (**I17**) reacts with **R12** via **TS23** to afford **P9**, **P11**, and (*S*)-**Cat2f**. Transition state **TS23** consists of simultaneous (i) C–S bond formation between the enol and **R12**, (ii) a H-shift from the O of the enol to the N of (*S*)-**Cat2f**, and (iii) a H-shift from the N of (*S*)-**Cat2f** to the N of **R12**. Subsequent reduction of **P9** with $NaBH_4$ will yield the experimentally observed product **P10**. The calculated reaction enthalpy profile is shown in Figure S8 (in Supplementary data).

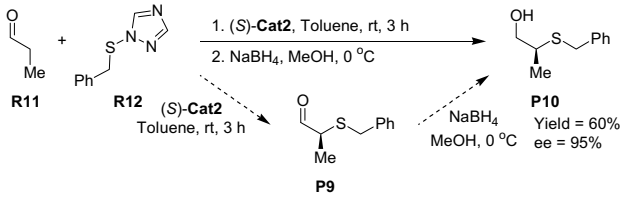

Scheme 19. (*S*)-**Cat2**-catalyzed α-sulfenylation of propanal.[1c]

3.7. α-Bromination of an aldehyde (C–Br bond formation)

The (*S*)-**Cat2**-catalyzed α-bromination of 3-methylbutanal (**R13**) with **R14** affords **P13** after $NaBH_4$ reduction (Scheme 21). The first-formed product (prior to $NaBH_4$ reduction) is expected to be **P12**. Following our proposed enol mechanism (Scheme 22), the *trans* enol–catalyst complex (**I18**) reacts with **R14** via **TS25** to afford **P12** and **I19**. Transition state **TS25** consists of simultaneous (i) C–Br bond formation between the enol and **R14** via a Br-shift, and (ii) a H-shift from the O of the enol to the N of (*S*)-**Cat2g**. Subsequent reduction of **P12** with $NaBH_4$ will yield the experimentally observed product **P13**. The calculated reaction enthalpy profile is shown in Figure S9 (in Supplementary data).

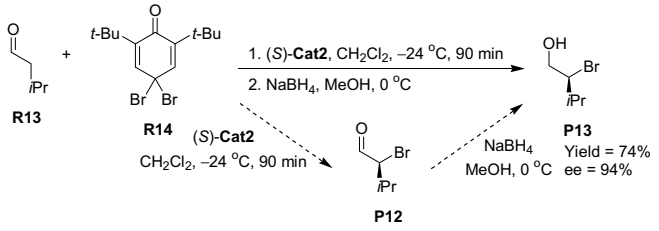

Scheme 21. (*S*)-**Cat2**-catalyzed α-bromination of aldehyde **R13**.[1c]

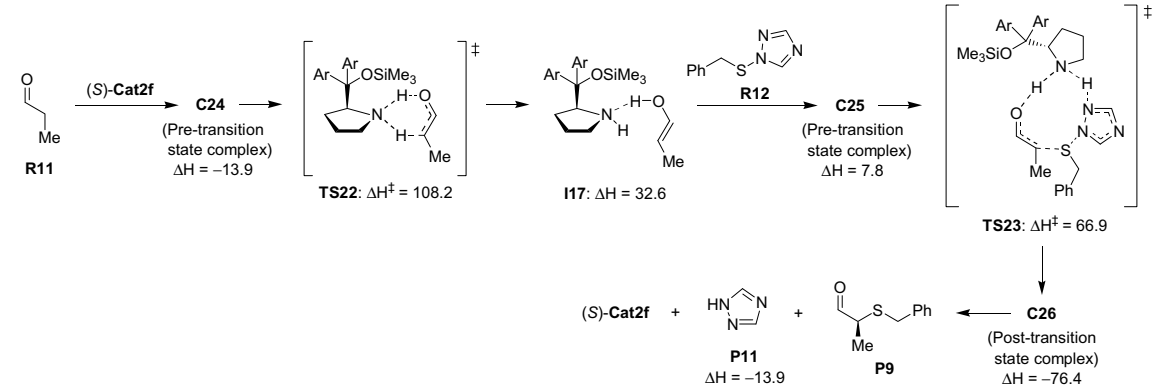

Scheme 20. Proposed reaction mechanism for the (*S*)-**Cat2f**-catalyzed α-sulfenylation of propanal, via an enol intermediate. Calculated enthalpy energies ($\Delta H^{\ddagger}$ and ΔH) correspond to the relative energy with respect to **R11** (i.e., the free reactants), in kJ mol^{-1}.

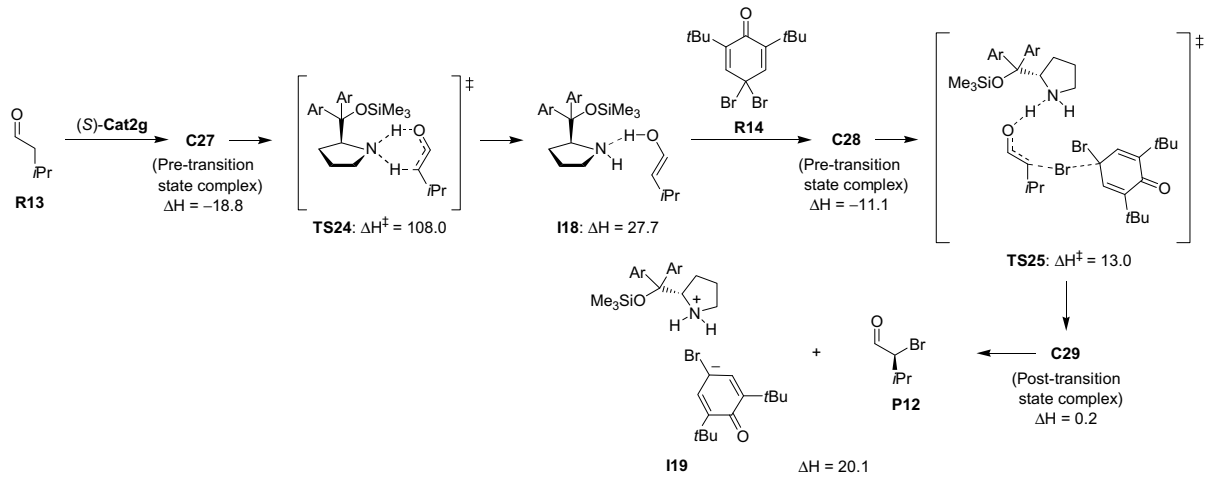

Scheme 22. Proposed reaction mechanism for the (*S*)-**Cat2g**-catalyzed α-bromination of 3-methylbutanal, via an enol intermediate. Calculated enthalpy energies ($\Delta H^{\ddagger}$ and ΔH) correspond to the relative energy with respect to **R13** (i.e., the free reactants), in kJ mol^{-1}.

4. Conclusion

We have investigated the enantioselectivity of the α,α-diarylprolinol trimethylsilyl ether-catalyzed C–C, C–N, C–F, C–S, and C–Br bond forming reactions by utilizing a proposed enol mechanism. In all the reactions considered, the proposed enol mechanism can fully account for the experimentally observed product enantioselectivity and diastereoselectivity. The α,α-diarylprolinol trimethylsilyl ether class of catalyst has been used for the α-functionalization of aldehydes with various different electrophiles, with consistently high levels of selectivity and the same product enantiomer. This suggests that a common intermediate is likely. Our study thus far strongly suggests that this intermediate is the enol and not an enamine.

Acknowledgements

We thank Bee Ling Kee for helpful discussions.

Supplementary data

Origin of diastereoselectivity, conformational flexibility of intermediates and transition states, calculated Gibbs free energy barriers, Cartesian coordinates, and absolute energies of all compounds. Supplementary data associated with this article can be found in the online version, at doi:10.1016/j.tet.2009.07.008.

References and notes

1. (a) Hong, B.-C.; Nimje, R. Y.; Sadani, A. A.; Liao, J.-H. *Org. Lett.* **2008**, *10*, 2345; (b) Palomo, C.; Vera, S.; Velilla, I.; Mielgo, A.; Gomez-Bengoa, E. *Angew. Chem., Int. Ed.* **2007**, *46*, 8054; (c) Franzen, J.; Marigo, M.; Fielenbach, D.; Wabnitz, T. C.; Kjærsgaard, A.; Jorgensen, K. A. *J. Am. Chem. Soc.* **2005**, *127*, 18296.
2. (a) Verkade, J. M. M.; Hemert, L. J. C.; Quaedflieg, P. J. L. M.; Rutjes, F. P. J. T. *Chem. Soc. Rev.* **2008**, *37*, 29; (b) Rueping, M.; Merino, E.; Sugiono, E. *Adv. Synth. Catal.* **2008**, *350*, 2127; (c) Gaunt, M. J.; Johansson, C. C. C.; McNally, A.; Vo, N. T. *Drug Discov. Today* **2007**, *12*, 8; (d) Gotoh, H.; Ishikawa, H.; Hayashi, Y. *Org. Lett.* **2007**, *9*, 5307; (e) Gotoh, H.; Hayashi, Y. *Org. Lett.* **2007**, *9*, 2859; (f) Guillena, G.; Ramon, D. J. *Tetrahedron: Asymmetry* **2006**, *17*, 1465; (g) Ibrahem, I.; Cordova, A. *Chem. Commun.* **2006**, 1760.
3. (a) Cabrera, S.; Reyes, E.; Aleman, J.; Milelli, A.; Kobbelgaard, S.; Jorgensen, K. A. *J. Am. Chem. Soc.* **2008**, *130*, 12031; (b) Melchiorre, P.; Marigo, M.; Carlone, A.; Bartoli, G. *Angew. Chem., Int. Ed.* **2008**, *47*, 6138; (c) Cabrera, S.; Aleman, J.; Bolze, P.; Bertelsen, S.; Jorgensen, K. A. *Angew. Chem., Int. Ed.* **2008**, *47*, 121; (d) Franke, P. T.; Richter, B.; Jorgensen, K. A. *Chem.—Eur. J.* **2008**, *14*, 6317; (e) Zhao, G.-L.; Vesely, J.; Rios, R.; Ibrahem, I.; Sunden, H.; Cordova, A. *Adv. Synth. Catal.* **2008**, *350*, 237; (f) Bertelsen, S.; Johansen, R. L.; Jorgensen, K. A. *Chem. Commun.* **2008**, 3016; (g) Reyes, E.; Jiang, H.; Milelli, A.; Elsner, P.; Hazell, R. G.; Jorgensen, K. A. *Angew. Chem., Int. Ed.* **2007**, *46*, 9202; (h) Hayashi, Y.; Pkano, T.; Aratake, S.; Hazelard, D. *Angew. Chem., Int. Ed.* **2007**, *46*, 4922; (i) Enders, D.; Huttl, M. R. M.; Grondal, C.; Raabe, G. *Nature* **2006**, *441*, 861; (j) Gotoh, H.; Masui, R.; Ogino, H.; Shoji, M.; Hayashi, Y. *Angew. Chem., Int. Ed.* **2006**, *45*, 6853.
4. (a) Shaikh, R. R.; Mazzanti, A.; Petrini, M.; Bartoli, G.; Melchiorre, P. *Angew. Chem., Int. Ed.* **2008**, *47*, 8707; (b) Enders, D.; Wang, C.; Bats, J. W. *Angew. Chem., Int. Ed.* **2008**, *47*, 7539; (c) Mielgo, A.; Palomo, C. *Chem. Asian J.* **2008**, *3*, 922; (d) Franke, P. T.; Johansen, R. L.; Bertelsen, S.; Jorgensen, K. A. *Chem. Asian J.* **2008**, *3*, 216; (e) Pellissier, H. *Tetrahedron* **2007**, *63*, 9267; (f) Ting, A.; Schaus, S. E. *Eur. J. Org. Chem.* **2007**, 5797; (g) Zhao, G.-L.; Cordova, A. *Tetrahedron Lett.* **2006**, *47*, 7417.
5. (a) Diner, P.; Kjærsgaard, A.; Lie, M. A.; Jorgensen, K. A. *Chem.—Eur. J.* **2008**, *14*, 122; (b) Shinisha, C. B.; Sunoj, R. B. *Org. Biomol. Chem.* **2008**, *6*, 3921.
6. (a) *Modern Aldol Reactions*; Mahrwald, R., Ed.; Wiley-VCH: Weinheim, 2004; Vols. 1 and 2; (b) Palomo, C.; Oiarbide, M.; Garcia, J. M. *Chem.—Eur. J.* **2002**, *8*, 36.
7. (a) List, B.; Hoang, L.; Martin, H. J. *Proc. Natl. Acad. Sci. U.S.A.* **2004**, *101*, 5839; (b) Hoang, L.; Bahmanyar, S.; Houk, K. N.; List, B. *J. Am. Chem. Soc.* **2003**, *125*, 16.
8. (a) Fu, A.; Li, H.; Si, H.; Yuan, S.; Duan, Y. *Tetrahedron: Asymmetry* **2008**, *19*, 2285; (b) Clemente, F. R.; Houk, K. N. *Angew. Chem., Int. Ed.* **2004**, *43*, 5766; (c) Bahmanyar, S.; Houk, K. N.; Martin, H. J.; List, B. *J. Am. Chem. Soc.* **2003**, *125*, 2475; (d) Rankin, K. N.; Gauld, J. W.; Boyd, R. J. *J. Phys. Chem. A* **2002**, *106*, 5155; (e) Arno, M.; Domingo, L. R. *Theor. Chem. Acc.* **2002**, *108*, 232; (f) Bahmanyar, S.; Houk, K. N. *J. Am. Chem. Soc.* **2001**, *123*, 11273; (g) Bahmanyar, S.; Houk, K. N. *J. Am. Chem. Soc.* **2001**, *123*, 12911.
9. Yalalov, D. A.; Tsogoeva, S. B.; Shubina, T. E.; Martynova, I. M.; Clark, T. *Angew. Chem., Int. Ed.* **2008**, *47*, 6624.
10. Wong, C. T. *Tetrahedron Lett.* **2009**, *50*, 811.
11. (a) Lee, C.; Yang, W.; Parr, R. G. *Phys. Rev. B* **1988**, *37*, 785; (b) Becke, A. D. *J. Chem. Phys.* **1993**, *98*, 5648.
12. (a) Cances, E.; Mennucci, B.; Tomasi, J. *J. Chem. Phys.* **1997**, *107*, 3032; (b) Mennucci, B.; Tomasi, J. *J. Chem. Phys.* **1997**, *106*, 5151; (c) Mennucci, B.; Cances, E.; Tomasi, J. *J. Phys. Chem. B* **1997**, *101*, 10506; (d) Cossi, M.; Barone, V.; Mennucci, B.; Tomasi, J. *Chem. Phys. Lett.* **1998**, *286*, 253; (e) Tomasi, J.; Mennucci, B.; Cances, E. *J. Mol. Struct. (Theochem)* **1999**, *464*, 211; (f) Cossi, M.; Scalmani, G.; Rega, N.; Barone, V. *J. Chem. Phys.* **2002**, *117*, 43.
13. Wong, M. W. *Chem. Phys. Lett.* **1996**, *256*, 391.
14. Frisch, M. J.; Trucks, G. W.; Schlegel, H. B.; Scuseria, G. E.; Robb, M. A.; Cheeseman, J. R.; Montgomery, J. A., Jr.; Vreven, T.; Kudin, K. N.; Burant, J. C.; Millam, J. M.; Iyengar, S. S.; Tomasi, J.; Barone, V.; Mennucci, B.; Cossi, M.; Scalmani, G.; Rega, N.; Petersson, G. A.; Nakatsuji, H.; Hada, M.; Ehara, M.; Toyota, K.; Fukuda, R.; Hasegawa, J.; Ishida, M.; Nakajima, T.; Honda, Y.; Kitao, O.; Nakai, H.; Klene, M.; Li, X.; Knox, J. E.; Hratchian, H. P.; Cross, J. B.; Adamo, C.; Jaramillo, J.; Gomperts, R.; Stratmann, R. E.; Yazyev, O.; Austin, A. J.; Cammi, R.; Pomelli, C.; Ochterski, J. W.; Ayala, P. Y.; Morokuma, K.; Voth, G. A.; Salvador, P.; Dannenberg, J. J.; Zakrzewski, V. G.; Dapprich, S.; Daniels, A. D.; Strain, M. C.; Farkas, O.; Malick, D. K.; Rabuck, A. D.; Raghavachari, K.; Foresman, J. B.; Ortiz, J. V.; Cui, Q.; Baboul, A. G.; Clifford, S.; Cioslowski, J.; Stefanov, B. B.; Liu, G.; Liashenko, A.; Piskorz, P.; Komaromi, I.; Martin, R. L.; Fox, D. J.; Keith, T.; Al-Laham, M. A.; Peng, C. Y.; Nanayakkara, A.; Challacombe, M.; Gill, P. M. W.; Johnson, B.; Chen, W.; Wong, M. W.; Gonzalez, C.; Pople, J. A. *Gaussian 03, Revision C.01*; Gaussian: Wallingford CT, 2004.
15. (a) Denmark, S. E.; Griedel, B. D.; Coe, D. M.; Schnute, M. E. *J. Am. Chem. Soc.* **1994**, *116*, 7026; (b) Gung, B. W.; Zhu, Z.; Fouch, R. A. *J. Org. Chem.* **1995**, *60*, 2860; (c) Wong, C. T.; Wong, M. W. *J. Org. Chem.* **2005**, *70*, 124.
16. Marigo, M.; Fielenbach, D.; Braunton, A.; Kjærsgaard, A.; Jorgensen, K. A. *Angew. Chem., Int. Ed.* **2005**, *44*, 3703.